Accepted Manuscript

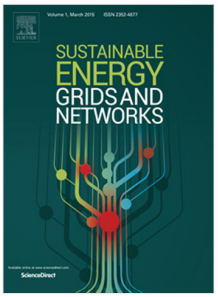

Misoperation analysis of steady-state and transient methods on earth fault locating in compensated distribution networks

Konstantin Pandakov, Hans Kristian Høidalen, Jorun Irene Marvik

PII: S2352-4677(16)30173-4
DOI: https://doi.org/10.1016/j.segan.2017.12.001
Reference: SEGAN 126

To appear in: *Sustainable Energy, Grids and Networks*

Received date : 29 November 2016
Revised date : 11 September 2017
Accepted date : 6 December 2017

Please cite this article as: K. Pandakov, H.K. Høidalen, J.I. Marvik, Misoperation analysis of steady-state and transient methods on earth fault locating in compensated distribution networks, *Sustainable Energy, Grids and Networks* (2017), https://doi.org/10.1016/j.segan.2017.12.001

Misoperation analysis of steady-state and transient methods on earth fault locating in compensated distribution networks

Konstantin Pandakov[a,1], Prof. Hans Kristian Høidalen[a,2], Dr. Jorun Irene Marvik[b,3]

[a] *NTNU, Norway, Trondheim 7491, O.S. Bragstads plass 2*
[b] *SINTEF Energy Research, Norway, Trondheim 7034, Sem Sælands vei 11*

Abstract

Earth fault detection and location are very important issues in distribution networks. Current methods for faulty feeder selection are based on measurements of steady-state or transient signals. The work presented here identifies and gives analyses of scenarios when ground protection based on these methods is prone to misoperation in resonance grounded systems. It is shown that the traditional watt-metric approach can malfunction depending on network and fault parameters. The admittance methods help to eliminate many issues, however they might have complex settings depending on network configurations. Special attention is paid to approaches based on transient signals as the most promising alternative solution. The current work considers methods utilizing zero sequence current, angle, power, energy and admittance transients. The paper reveals limitations for their application mainly due to presence of electrostatic asymmetry, cables in a network, fault resistance and inception angle. Nevertheless, dependability of these methods is higher than the steady-state especially for intermittent faults. It is also found that analysis of prefault information is important both for the steady-state and the transient methods. The obtained results can be used to enhance reliability of protective schemes and as drivers

[1]Corresponding author, email: konstantin.pandakov@ntnu.no
[2]Co-authors-1, email: hans.hoidalen@elkraft.ntnu.no
[3]Co-authors-2, email: jorun.irene.marvik@sintef.no

for further developments of new algorithms.

Keywords: ground fault protection, resonant grounding, transient method, watt-metric

1. Introduction

From the current operation practice of medium voltage (MV) networks, it is well known that the vast majority of faults are single-line-to-earth type. In order to decrease fault current, a system can be operated as an isolated or a non-solidly earthed. In this work, the special type of grounding of the main distribution transformer is considered – through a Petersen coil that is quite common in Nordic countries. In resonance grounded systems, ground faults are easily detected (apart from high impedance faults) by measuring the zero sequence voltage magnitude $|\bar{U}_0|$ (exceeds thresholds at a substation), and fault current is suppressed facilitating self-extinguishing of the arc.

For permanent faults, in order to affect as few customers as possible, it is necessary to find the faulty point in the system and isolate it. Measured $|\bar{U}_0|$ does not significantly depend on fault location in a network; moreover, fault current is comparable with load currents that also jeopardizes selectivity of the protection. Typically, problem of faulty feeder selection is considered and X. Zhang et al. [1] provide comprehensive review on the developed methods for this purpose. They can be divided into three groups: injection of additional signals in a substation (voltage, current with frequencies equal to fundamental or higher), usage of steady-state signals, and utilization of transients arising during faults. The injecting methods require additional equipment and they are out of the scope of this paper.

The traditional way of faulty feeder selection based on steady-state signals is the watt-metric approach [1]: detection of a magnitude and direction of zero sequence current $\bar{I}_0$ with respect to $\bar{U}_0$ – normally, healthy feeders and a faulty have different quadrants and magnitudes. In other words, $|\bar{I}_0|\cos(\phi_0)$ (where zero sequence angle ϕ_0 is between $\bar{U}_0$ and $\bar{I}_0$) will have a different sign for a faulty

feeder comparing to a healthy. Thus, directionality of the ground protection is tuned according to this fact.

Paper [2] describes insufficiency of the watt-metric approach and a need for a resistor connected in parallel to a Petersen coil. Such operation leads to increase of fault current, produces transient overvoltages in a grid and it requires additional equipment; therefore, it is of interest to find new approaches. In case of sufficient line-to-ground conductance and arcing faults (small impedances), $|\bar{I}_0|\cos(\phi_0)$ can be applied without the resistor. Nevertheless, reference [3] reports the special cases when the sign of $|\bar{I}_0|\cos(\phi_0)$ in both a healthy and a faulty feeders are opposite compared to the prescribed polarity that can lead to misoperation of relays. It is also worth mentioning that a magnitude of zero sequence current by itself is not a reliable indicator for high impedance faults or presence of cables in a system. A new steady-state solution, in contrast to the watt-metric approach, based on zero sequence admittance is proposed in [4]. It copes with lose of sensitivity and other issues.

As an alternative, transient methods are becoming a promising solution. In addition to what was given in [1], authors of [5, 6] suggest to utilize the shape of the charge-voltage curves. In [7, 8] deviation of the feeder capacitance to the ground is estimated. Paper [9] suggests to measure only phase current with further detection of its relative change with respect to the previous periods. Besides the wavelet analysis, other approaches are also performed, such as the Hilbert-Huang [10] and the S-transform [11] investigations. Authors of [12] describe research on the frequency spectrum. The artificial intelligence algorithms involving the fuzzy-logic [13], application of the analytic hierarchy process [14] and the small-world network theory [15] can be found in literature as well.

The first-half-wave methods [1] based on low frequency transients deserve special attention due to suitability for compensated and isolated systems, and practical realization connected with limited sampling frequencies (few kilohertz) of used modern relays. High frequency transients might be contaminated by noise from measuring devices that makes application of associated methods difficult. The basic idea behind the first-half-wave methods is different polarity of

instantaneous zero sequence current i_0 (with respect to voltage u_0) of a faulty feeder in comparison with other right after fault inception that helps to make decision in the first half of a period. Paper [16] illustrates this effect and proposes the algorithm calculating zero sequence impedance through averaged over a specified time window quantities. Authors of [17] utilize simple differential of i_0 (calculated at the first milliseconds) for faulty feeder selection. References [18, 19] present extraction of transient ϕ_0 and application of it as a main indicator. In order to enhance dependability, different summation and integration techniques are proposed. For instance, papers [20, 21, 22] calculate zero sequence active power over a quarter of the period, [23] – energy (integration time is not specified). In contrast, the Cumulative Phasor Summing (CPS) technique of zero sequence admittance for different moments of a transient period is used in [24].

To summarize, effect of difference between the prescribed and a factual sign of $\cos(\phi_0)$ in a faulty feeder illustrated in [3] is a key factor leading to inadequacy of ground protection based on the watt-metric approach. As the nature of this effect has not been analyzed in literature in details, the first contribution of the current paper is a deep analysis of it. Moreover, the paper shows how the effect might jeopardize the steady-state [4] and even transient methods. From the variety of the transient methods, the paper will substantially deal with the basic approaches utilizing transients of zero sequence current [16], angle [19], energy [23], and admittance [24]. As it is slightly mentioned in [1], the transient methods are vulnerable to network and fault parameters; therefore, several adverse effects deteriorating performance of the algorithms have not been revealed in the prior studies due to simplicity of the models (e.g. ideal symmetry) and lack of simulation cases. Hence, the next contribution of the paper is revealing what network nonidealities and fault origins can affect performance of ground relays based on these transient methods. The presented results might be valuable for estimation of the limitations of the methods both in relay planning in compensated distribution systems and as background for developments of new algorithms.

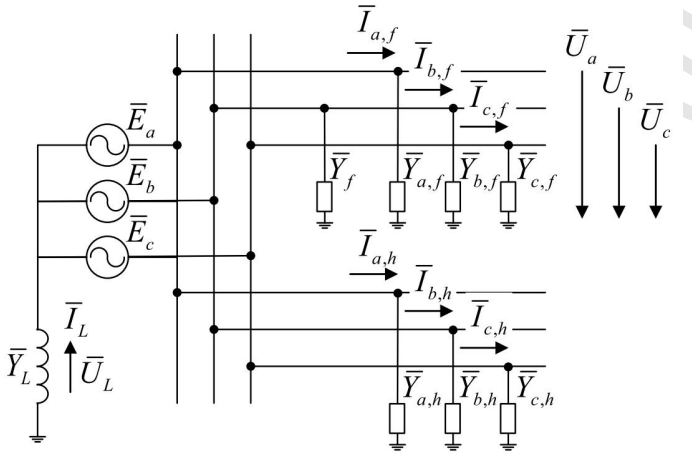

Figure 1: Simplified network for analysis with two feeders.

2. Theoretical analysis on fault locating utilizing steady-state signals

Let us consider a simple network depicted in Fig.1 with the ground fault in phase b of the upper feeder.

The network parameters: $\bar{Y}_{a,f} = \bar{Y}_{c,f} = k_f\bar{Y} = k_f(G + j\omega C)$, where $k_f\bar{Y}$ expresses the share of the faulty feeder in the total shunt admittance to the ground of the network per phase, $\bar{Y}$, that consist of conductance G and capacitance C of a phase. Similarly, $\bar{Y}_{a,h} = \bar{Y}_{c,h} = (1 - k_f)\bar{Y} = k_h\bar{Y}$. Indices f and h in the paper denote the faulty and the healthy feeder correspondingly. MV networks have capacitive imbalance $\Delta\bar{Y} = j\omega\Delta C$ that is normally 1-5% from $3\bar{Y}$ [25]. Let us assume that it takes place in phase b, then $\bar{Y}_{b,f} = k_f(\bar{Y} + \Delta\bar{Y})$ and $\bar{Y}_{b,h} = k_h(\bar{Y} + \Delta\bar{Y})$. The fault impedance is assumed to be pure resistive, $\bar{Y}_f = G_F$. In this work, only permanent resistive fault is studied.

For simplified steady-state analysis of ground faults, series impedances of transmission lines and loads can be neglected in comparison with large shunt impedances of lines. Taking this into account, the following set of equations can be written to describe the system in steady-state conditions:

$$\begin{cases} 3\bar{I}_{0,h} = 3\bar{U}_0 k_h \bar{Y} + \bar{U}_b k_h \Delta\bar{Y} \\ 3\bar{I}_{0,f} = 3\bar{U}_0 k_f \bar{Y} + \bar{U}_b k_f \Delta\bar{Y} + \bar{U}_b G_F \\ \bar{I}_L = 3\bar{I}_{0,f} + 3\bar{I}_{0,h} \\ \bar{E}_{ph} = \bar{U}_{ph} + \bar{U}_L \\ \bar{I}_L = \bar{Y}_L \bar{U}_L = -\bar{Y}_L \bar{U}_0 \end{cases}, \quad (1)$$

where index ph stands for phases a, b and c; $\bar{U}_{ph}$ – phase voltage; $\bar{E}_{ph}$ – the balanced source of voltage; $\bar{I}_L$ and $\bar{U}_L$ are current and voltage of the Petersen coil, and $\bar{Y}_L = (j\omega L)^{-1}$ its admittance; zero sequence voltage and currents are determined as $3\bar{U}_0 = \sum \bar{U}_{ph}$ and $3\bar{I}_{0,f/h} = \sum \bar{I}_{ph,f/h}$.

Let us assume for simplicity that $k_f = k_h$, then the second equation in (1) is turned to $3\bar{I}_{0,f} = 3\bar{I}_{0,h} + \bar{U}_b G_F$. The phasor diagram for this case can be found in Fig.2a ($\Delta\bar{Y}$ is 1%, direction of zero sequence current is from the substation).

As it is possible to see, ϕ_0 of the healthy feeder is less than 90^0 ($|\bar{I}_{0,h}|\cos(\phi_{0,h}) > 0$) and vice versa for the faulty feeder ($|\bar{I}_{0,f}|\cos(\phi_{0,f}) < 0$). The traditional ground protection is based on this fact. It should also be noticed that such systems in Norway are overcompensated, therefore in further analyses $|\bar{Y}_L| > 3|\bar{Y}|$. After fault identification, a resistor can be connected in parallel with the coil that increases ϕ_0 in the faulty feeder and helps to facilitate the selection if watt-metric contribution is scarce.

Now, let us assume that $\Delta\bar{Y}$ is 5% in the network (it provokes decrease of $\bar{U}_L$ and $\bar{I}_L$ to preserve the same compensation rate). The phasor diagram for this case is illustrated in Fig.2b. The zero sequence currents for both feeders change the quadrants: apart from the previous case, $|\bar{I}_{0,f}|\cos(\phi_{0,f}) > 0$ and $|\bar{I}_{0,h}|\cos(\phi_{0,h}) < 0$. The protection can misjudge the healthy feeder as the faulty that is referred to as polarity disruption of ground relays. A parallel resistor will aggravate the situation. Authors of [3] showed through simulations that such situation appears for faults in a phase with the biggest capacitance. As a matter of fact, it can also occur in other phases depending on network and

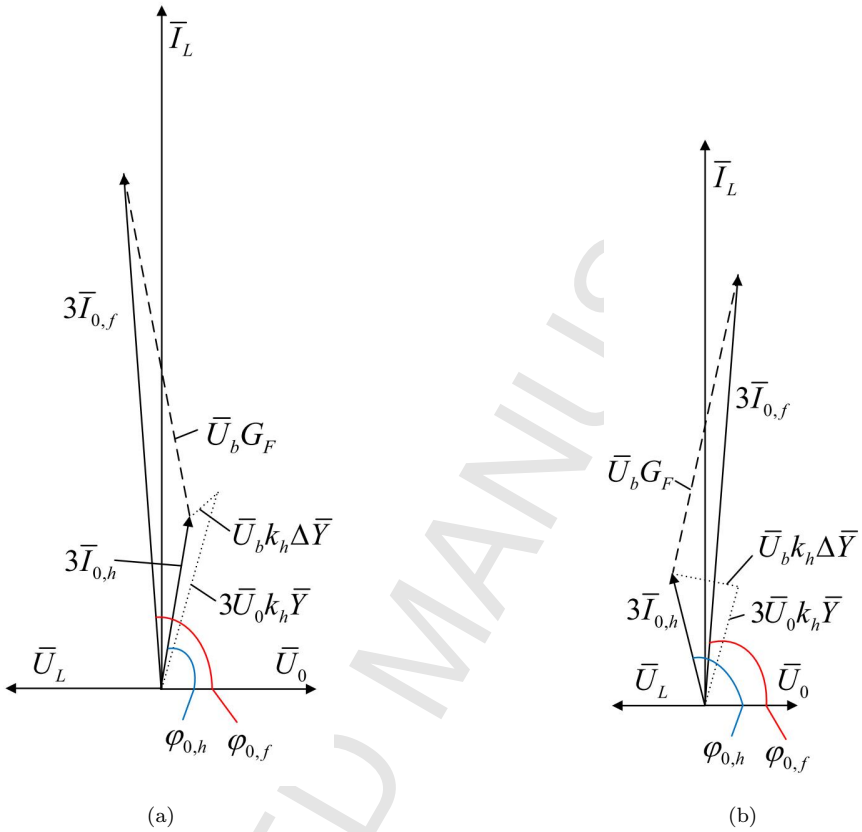

Figure 2: Phasor diagram of the simplified network for fault in phase b and a) $\Delta\bar{Y} = 1\%$, b) $\Delta\bar{Y} = 5\%$.

fault parameters, therefore this effect requires more thorough investigation.

2.1. Analysis of the polarity disruption

Finding of dependencies of the performed effect on network and fault parameters can be derived analytically through solution of (1) and decompositions of an angle of $\bar{I}_{0,h/f}/\bar{U}_0$ into real and imaginary parts. Here, numerical sensitivity analysis is performed with the following parameters (the base is 22 kV and 20 MVA): $|\bar{E}_{ph}| = 1$ p.u., $\bar{Y} = (0.24 + j6.64) \cdot 10^{-3}$ p.u. and $k_f = k_h$.

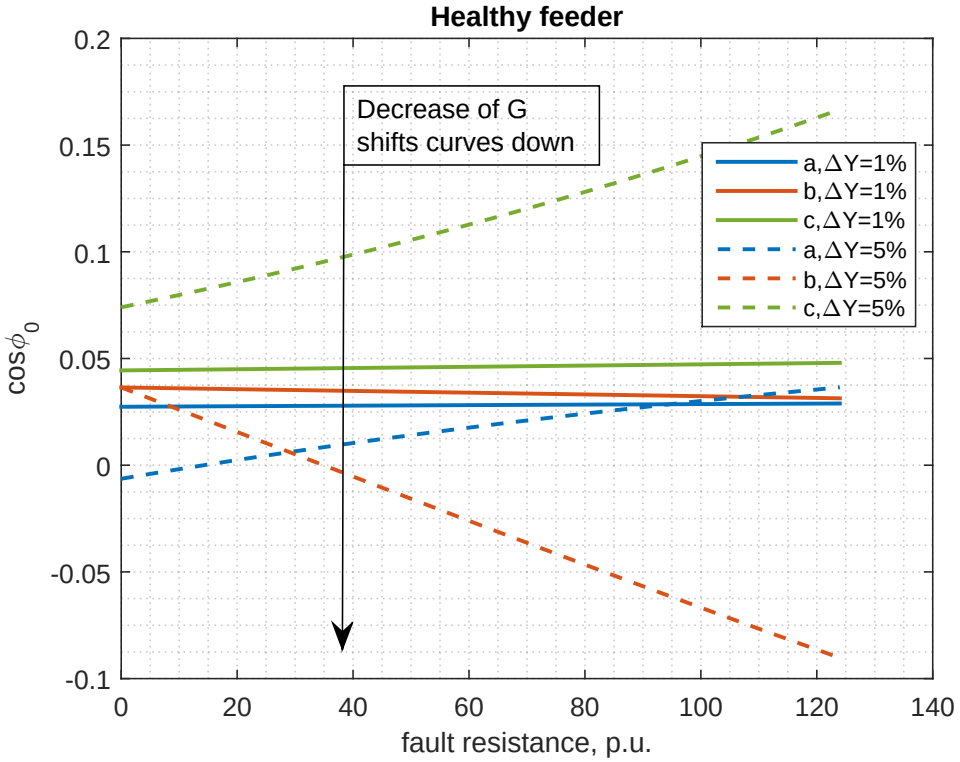

Figure 3: Dependency of $\cos(\phi_0)$ on fault resistance in healthy feeder for fault in different phases, $\Delta\bar{Y} = 1\%$ and 5%, fixed compensation rate.

It is possible to get from (1) that

$$\bar{U}_0 = \frac{\bar{E}_b \Delta\bar{Y} + \bar{E}_b G_F}{-\bar{Y}_L - 3\bar{Y} - \Delta\bar{Y} - G_F} \tag{2}$$

Assuming $G_F = 0$ as prefault conditions and choosing overcompensation rate $K = |\bar{U}_0/\bar{E}_b|$ as 5% [25] (hereafter, such definition is used), inductance of the coil can be calculated for different network parameters. Having $\bar{U}_0$ for fault conditions ($G_F \neq 0$), cosine of angle of $\bar{I}_{0,h/f}/\bar{U}_0$ can be determined.

Fig.3 shows the results of analysis for constant compensation rate: dependency of $\cos(\phi_0)$ on fault resistance for three phases and different capacitive imbalance (1% and 5%).

From the plot, it can be seen that dependencies are not prominent for the

small $\Delta\bar{Y}$, whereas more evident for the high imbalance. It must be noted that insufficiency of watt-metric contribution (small G) shifts all curves down. Taking this fact and the dependencies into account, it is possible to conclude that probability of relay misoperation in the healthy feeder ($\cos(\phi_{0,h}) < 0$) increases with rise of fault resistance for phase b and decreases for a and c. The same conclusions are valid for the faulty feeder.

Fig.4 demonstrates the results for variation of compensation rate. It is observable from the upper plot (the small fault resistance) that $\cos(\phi_{0,h}) < 0$ only occurs for phase a and $\Delta\bar{Y} = 5\%$. Nevertheless, all curves might fall into the negative half-plane in case of insignificant G. The dependencies are more nonlinear for the high fault resistance (the lower plot). As the curves are shifted down with decrease of G, then larger overcompensations (small L) might lead to misjudgment ($\cos(\phi_{0,h}) < 0$) for faults in phase b and increase dependability of ground protection for faults in phases a and c. It is seen that the opposite situation arises for higher L. Analysis for the faulty feeder demonstrates the same results.

From these conclusions, it is noticeable that reliability of the traditional steady-state approach is low for insignificant natural watt-metric contribution and high electrostatic imbalance. Moreover, dependency of the polarity disruption effect on network and fault parameters prejudices application of $|\bar{I}_0|\cos(\phi_0)$ for faulty feeder selection without the parallel resistor. The effect also has impact on the alternative admittance method [4]; therefore, full analysis including lines (with $k_f \neq k_h$) and loads follows.

3. Theoretical analysis of fault location utilizing transient signals

In this paper, signals are only analyzed at the fundamental frequency and all high frequency components are filtered out. For the system in Fig.1, the following set of equations is valid for the instantaneous quantities:

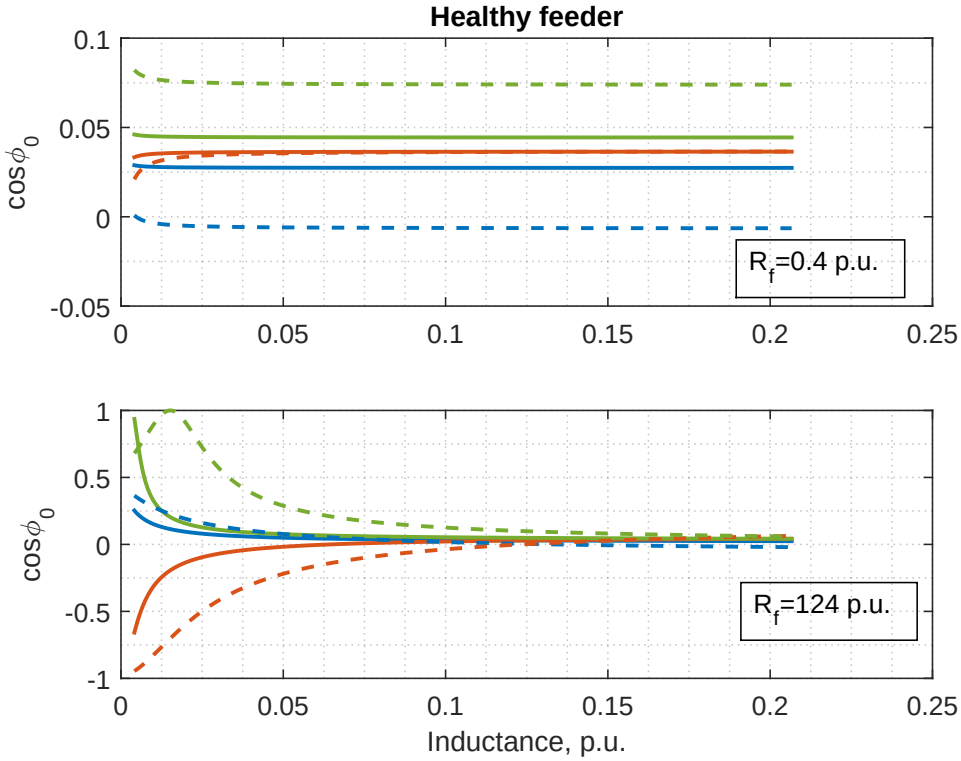

Figure 4: Dependency of $\cos(\phi_0)$ on inductance of the Petersen coil in healthy feeder for fault in different phases, $\Delta\bar{Y} = 1\%$ and 5%, two fixed fault resistances $R_f = 0.4$ p.u. and 124 p.u. The legend is the same as in Fig.3.

$$\begin{cases} 3i_{0,h} = 3\frac{du_0}{dt}k_hC + 3u_0k_hG + \frac{du_b}{dt}k_h\Delta C \\ 3i_{0,f} = 3\frac{du_0}{dt}k_fC + 3u_0k_fG + \frac{du_b}{dt}k_f\Delta C + u_bG_F \\ i_L = 3i_{0,f} + 3i_{0,h} \\ e_{ph} = u_{ph} + u_L \\ u_L = L\frac{di_L}{dt} = -u_0 \end{cases} \tag{3}$$

Numerical solution of this set, based on the Runge-Kutta method with time discretization 10^{-5} s, with the same parameters used before and $G_F = 0.008$ p.u., $\Delta\bar{Y} = 0.02 \cdot 3\bar{Y}$, $K = 5\%$ ($L = 0.113$ p.u.) is demonstrated in Fig.5 as

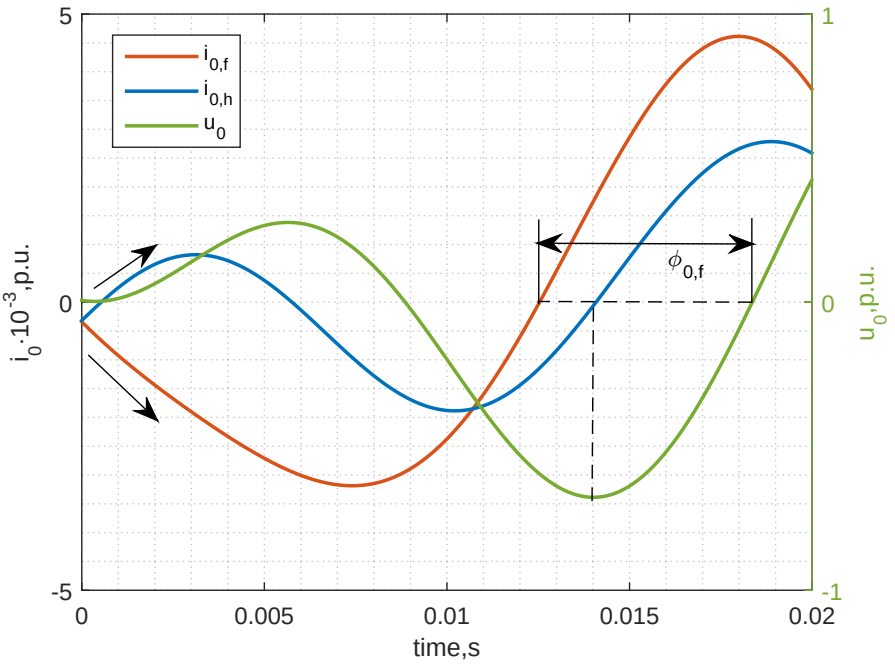

Figure 5: Numerical solution of the differential equations in (3) for zero sequence voltage u_0 and currents in healthy $i_{0,h}$ and faulty feeder $i_{0,f}$.

$u_0(t)$, $i_{0,f/h}(t)$. The initial conditions (in p.u.) corresponding to $u_b(0) = 0$: $e_a(0) = -1.222$, $e_b(0) = -0.006$, $e_c(0) = 1.228$, $u_0(0) = 0.006$, $i_L(0) = -1.98$.

The dynamic changes of the zero sequence currents in the faulty and the healthy feeder right after the fault ($t = 0$) are in opposite directions due to (dis)charging processes of the line capacitances. This peculiarities is used, for example, in the algorithm performed in [16]. Furthermore, considering the rest part of the transient period, it is seen that the zero sequence angle in the faulty feeder $\phi_{0,f}$ tends to values greater than 90^0. This phenomenon is used, for instance, in [19]. As a matter of fact, the transient period is significantly affected by network structures, parameters (including loads and line impedances), presenting nonidealities and fault origins; therefore, it requires further thorough investigation using an EMTDC-like software.

4. Test case network

The study is carried out based on the network depicted in Fig.6. The model is built in PSCAD$^{\text{TM}}$/EMTDC$^{\text{TM}}$. The main grid is modeled as an ideal voltage source with inductance (provides short circuit capacity). The distribution network consists of two feeders (transmission lines TL1, TL2 with variable lengths 10-50 km) with frequency dependent distributed parameters. For the given in Appendix A geometry, PSCAD calculates an admittance to the ground of each line per phase (per km) that gives possibility to determine the total network admittance per phase $\bar{Y}$. Electrostatic imbalance in the network $\Delta\bar{Y} = j\omega\Delta C$ is modeled as additional capacitors connected to phase b at the beginning and the end of each feeder; their values can be calculated as $k_{f/h}\Delta C/2$. Coefficients k_f and k_h will only depend on line lengths since their geometric parameters are the same, and $\Delta\bar{Y}$ is chosen as 1-5% from $3\bar{Y}$ to determine ΔC. The main distribution transformer has delta-wye connection and the secondary low voltage side is grounded by the inductor. L is varied in accordance with $3\bar{Y}$ and so that to get compensation rate $K = 1-5\%$ from phase voltage of the transformer secondary side. In order to exclude influence of mutual inductances between phases, the lines are ideally transposed. Other parameters can be found in Appendix A.

The ground fault is always applied in Feeder 1 at the end (the location on the feeder is fixed because its change will not significantly alter the results). Simulated voltages and currents (as in Fig.5) are processed through the Discrete Fourier Transform (one-cycle at 50 Hz, sampling frequency is 4 kHz) with low-pass filtering (second order Butterworth with 1.5 kHz cut-off frequency) in order to extract magnitudes and angles of the fundamental components only. Consequently, apart from instantaneous quantities, we obtain dynamic variation of $\bar{U}_0$ and $\bar{I}_0$ (time-varying 50 Hz phasors) for further analysis.

Models of current transformers are not included into this study; however, it must be noted that their accuracy might be a concern for small fault currents and, as a consequence, for the locating methods.

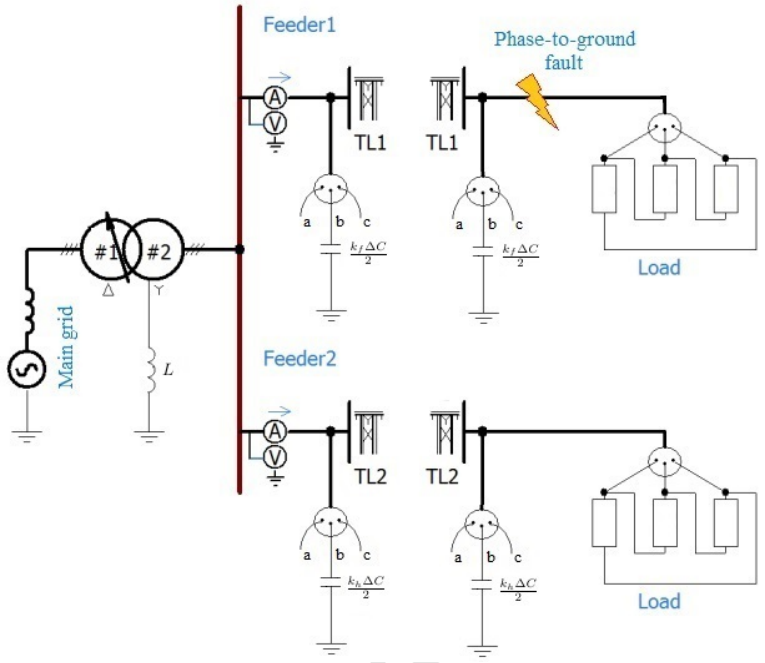

Figure 6: Test case network.

5. Results and discussions

5.1. Steady-state signals

Impact of variable network and fault parameters on the watt-metric approach has been studied using the performed model (for $k_f = k_h$). The results obtained through the simulations demonstrates similar dependencies of $\cos(\phi_{0,h})$ as in Fig.3 and Fig.4, and therefore are not presented. Additionally to the previous conclusions, it was found that load variation has indirect influence provoking changing of L in order to keep the same compensation rate; it can be regarded as the dependency on inductance in Fig.4. Finally, it was identified that ground resistivity does not have significant influence on performance of the steady-state methods.

The new admittance-based method described in [4] has been investigated for faulty feeder selection: the results are performed in Fig.7a ($k_f = k_h$, both lines

are 50 km). Zero sequence admittances $\bar{Y}_0 = (\bar{I}_0 - \bar{I}_{0\text{pre}})/(\bar{U}_0 - \bar{U}_{0\text{pre}}) = G_0 + jB_0$ ("pre" stands for prefault) are calculated for the faulty (the red markers) and the healthy feeder (the blue) for different network and fault conditions. As it is possible to see, the faulty admittances fall into the operating area for the faulty feeder irrespectively of phase, compensation, electrostatic imbalance, fault impedance or watt-metric contribution of the network.

Fig.7b shows the admittances calculated for $k_f \neq k_h$, fault resistance $R_f = 3$ kΩ, $\Delta\bar{Y}$ is 2%, $K = 5\%$. If the faulty feeder is shorter than the healthy (10 km versus 50 km, that is $k_f = 1/6$ and $k_h = 5/6$), $\bar{Y}_{0,f}$ is in the operating area (the red o–marker). If it is longer (50 km versus 10 km, that is $k_f = 5/6$, $k_h = 1/6$), $\bar{Y}_{0,h}$ falls into the operating area, whereas $\bar{Y}_{0,f}$ is in the non-operating (the x–markers). Such situation is present due to two reasons: firstly, it is the polarity disruption effect; secondly, prefault ϕ_0 displacements caused by $|\bar{I}_{0,f}| > |\bar{I}_{0,h}|$ (prefault) because $k_f > k_h$. This issue requires individual settings for each feeder with more complex operating area in order to avoid misoperation.

It has been found that for cases with $k_f \neq k_h$, the same conclusions regarding postfault $\cos(\phi_0)$ are applicable (Fig.3, Fig.4). Displacement of ϕ_0 must be taken into account if a method utilizes prefault measurements. This phenomenon is typical for a network with cables and will be illustrated later.

5.2. Transient signals

This section examines scenarios when the algorithms [16, 19, 23, 24] based on transient signals are prone to misoperation. Furthermore, two fault start times are applied: when phase voltage u_{ph} in faulty phase crosses 0 that is referred to as 0^0 inception angle (might occur when an extraneous object is in contact with a power line); when u_{ph} has a maximum value, that is 90^0 inception angle (can happen due to leakage ground current through an aged isolator). Below application of different quantities as an indicator of the faulty feeder is studied.

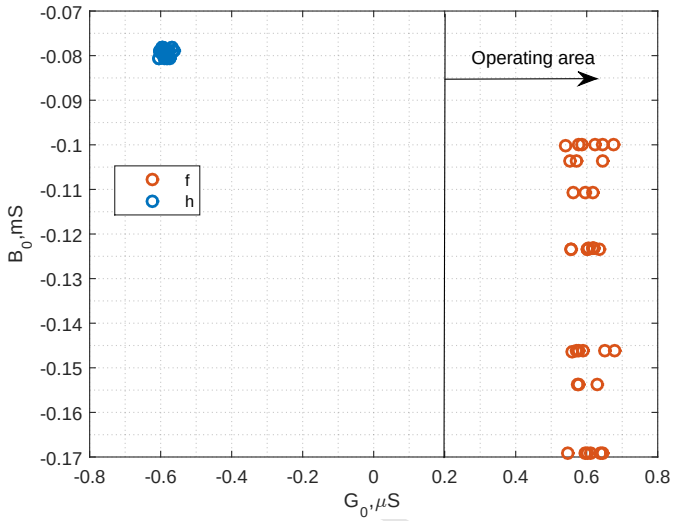

(a)

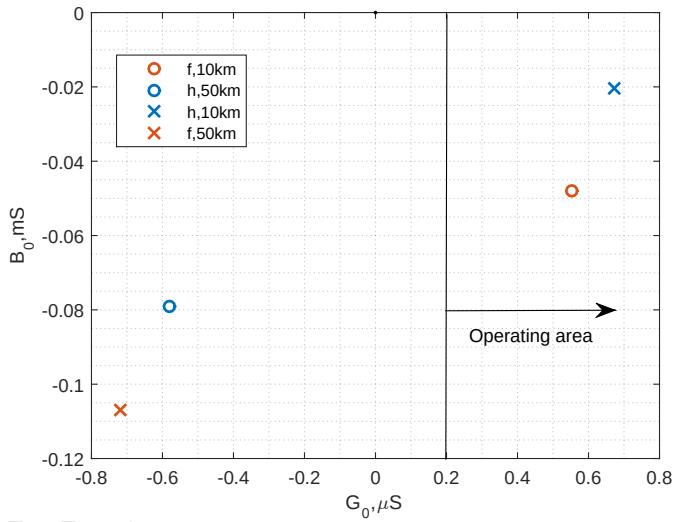

(b)

Figure 7: Calculated zero sequence admittances for (a) equal feeder lengths of 50 km, $k_f = k_h = 0.5$ and (b) different feeder lengths: $k_f = 1/6$, $k_h = 5/6$ and $k_f = 5/6$, $k_h = 1/6$.

5.2.1. Indicators based on zero sequence angle

Fig.8a shows the typical behavior of $\cos(\phi_0)$ in case of fault ($K = 5\%$, $R_f = 3$ kΩ, $\Delta\bar{Y} = 1\%$, 0^0 inception angle, both lines are 50 km) in the phase with small capacitance to the ground. The similar picture is observed for symmetrical systems regardless of a phase. Paper [19] suggests to use a simple threshold (the dashed line) to select the faulty feeder; however, it is not suitable solution in case of faults in the asymmetrical system: Fig.8b shows the transients for the same ground fault in phase b – $\cos(\phi_0)$ of the healthy and the faulty feeder cross the threshold.

Simulations have revealed that the transient process is not significantly affected by $\Delta\bar{Y}$, but extended penetration of $\cos(\phi_{0,h})$ into the negative half-plane mainly occurs for large K and phase a with 90^0 inception angle or b with 0^0 hindering the decision making procedure. Additionally, small fault resistances make the process faster (all important transients are only present during the first 5 ms) and oscillatory (change of the sign) that complicates signal acquisition and processing.

5.2.2. Indicators based on zero sequence energy

Paper [23] offers to use e_0 for feeder selection:

$$e_0 = \frac{1}{T}\int_{t_{inc}}^{t_{stop}} \int_{t-T}^{t} i_0(\tau)u_0(\tau)\mathrm{d}\tau, \tag{4}$$

where t_{inc} is time of fault inception, t_{stop} – time of the end of integration, T is the period of the fundamental component.

Such parameter can help to avoid uncertainties caused by variation of $\cos(\phi_0)$ during the transient process. Fig.9a illustrates the application of it for the same fault in phase b (Fig.8b) – e_0 of the faulty feeder develops into the negative half-plane as shown in [23]. Nevertheless, due to the polarity disruption effect appearing for high $\Delta\bar{Y}$, e_0 for the healthy and the faulty feeder can change the half-planes (the dashed curves). This effect can also jeopardize other methods based on power, energy, impedance or admittance calculations. Proper choice of t_{stop} might not improve the situation because, as it is shown in Fig.9b for

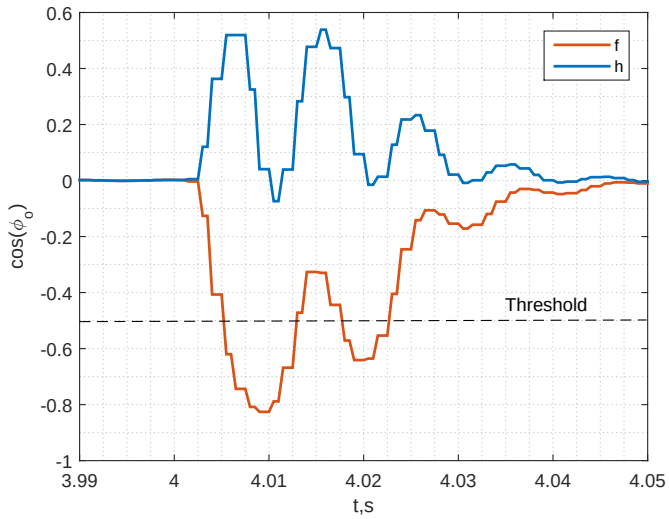

(a)

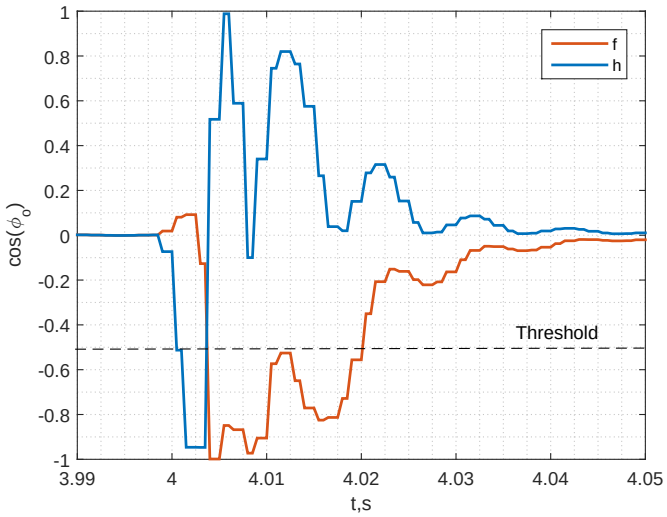

(b)

Figure 8: Transient characteristics of $\cos(\phi_0)$ for high impedance fault ($\Delta\bar{Y} = 1\%$, 0^0 inception angle) in phase a) *a*, b) *b*.

faults in phase *a* with 0^0 inception angle and $R_f = 10\ \Omega$, e_0 of the healthy feeder comes into the negative half-plane (and vice versa for he faulty) breaking the

preset polarity. The reason was shown in the theoretical analysis (Fig.3, Fig.4): $\cos(\phi_{0,h}) < 0$ occurs for phase a and low fault resistances. Additionally, it was found that the method is highly sensitive to correct determination of t_{inc} (error in 1 ms is sufficient to get the wrong decision because of phase oscillations) and requires different settings for relays. It was also shown by [3] that the polarity disruption has negative influence on this method in the steady-state period.

5.2.3. Indicators based on polarity of instantaneous zero sequence current

The method based on polarity of i_0 described in [16] shows correct operation in all cases above. Nevertheless, the approach is compromised for the system with an underground cable. In order to demonstrate this, the model (Fig.6) is modified as follows: Feeder 1 has a 25 km overhead line and a 25 km underground cable (the parameters are given in Appendix A) connecting the load and the line, length of TL2 is 50 km.

Fig.10 shows the normalized by the steady-state values instantaneous zero sequence currents and voltage for high impedance fault in Feeder 1. It is possible to see that right after the fault inception $di_{0,h}/dt < 0$ and $du_0/dt < 0$ as well; from the theoretical analysis and previous studies, $di_{0,f}/dt > 0$ must be true (as in Fig.5), whereas it is not regardless of inception angle (or phase) due to large capacitance to the ground of the cable. However, this effect is not present during faults in Feeder 2 (without cables) or low R_f.

It is worth mentioning that e_0 is not the reliable indicator for high impedance faults occurring at 90^0 inception angle for the given system because of strong capacitive current from the cable.

5.2.4. Indicators based on zero sequence admittance

The Cumulative Phasor Sum proposed in [24] is calculated as:

$$\Sigma\bar{Y}_0 = \sum_{i=t_{inc}}^{t_{stop}} \bar{Y}_0(i), \tag{5}$$

where $\bar{Y}_0(i) = \bar{I}_0(i)/\bar{U}_0(i)$ is the zero sequence admittance (the fundamental frequency is considered) at specific time instant i.

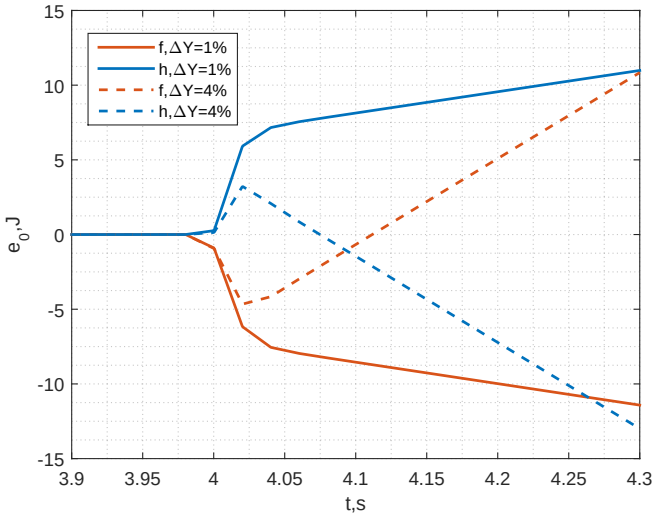

(a)

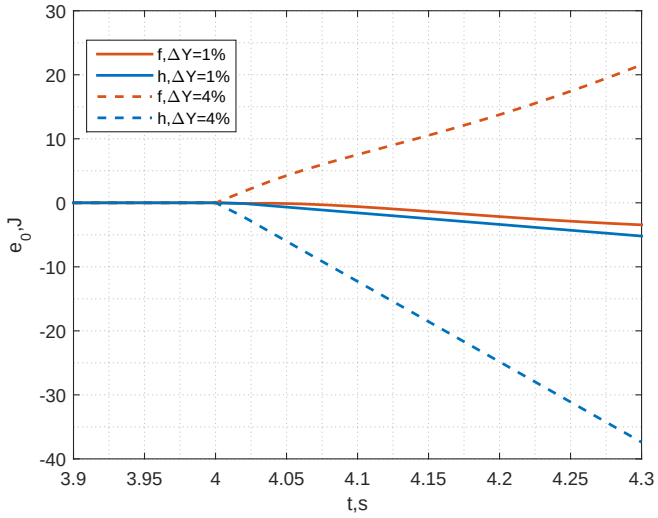

(b)

Figure 9: Zero sequence energy e_0 for fault in phase a) b with $R_f = 3$ kOhm, b) a with $R_f = 10$ Ohm, and different $\Delta\bar{Y}$.

With proper t_{stop} (otherwise $\Sigma\bar{Y}_0$ will have an opposite sign due to the polarity disruption effect), this method analogously demonstrates good performance

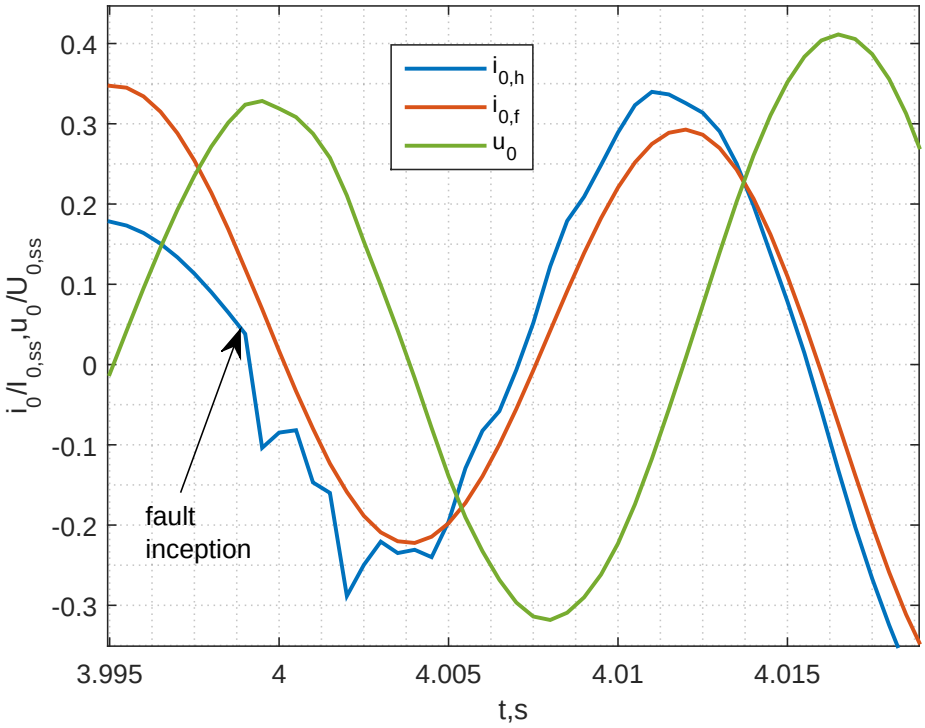

Figure 10: Normalized by steady-state values instantaneous u_0 and i_0 for high impedance fault in feeder with cable.

for cases in subsections 5.2.1 and 5.2.2. Moreover, it is fast (designed for intermittent faults) and does not require variety of settings – the decision is made on the ground of phasor positions. Nevertheless, an adverse effect appears for the system with the cable in subsection 5.2.3.

Fig.11 demonstrates extracted $\cos(\phi_0)$ for fault in phase a, $K = 3\%$, $\Delta\bar{Y} = 2\%$, 90^0 inception angle, $R_f = 10\ \Omega$ and $R_f = 3\ \text{k}\Omega$. Presence of the cable leads to significant inequality of prefault zero sequence currents in the feeders, $|\bar{I}_{0,f}| \gg |\bar{I}_{0,h}|$; therefore, as can be seen from the plot, there is displacement of prefault $\cos(\phi_0)$ of the healthy feeder mentioned in section 5.1. Due to this reason together with high $R_f = 3\ \text{k}\Omega$, faults in Feeder 1 will lead to $\cos(\phi_{0,h}) < 0$ during the transient and the steady-state periods. For $R_f = 10\ \Omega$, $\cos(\phi_{0,h})$ is

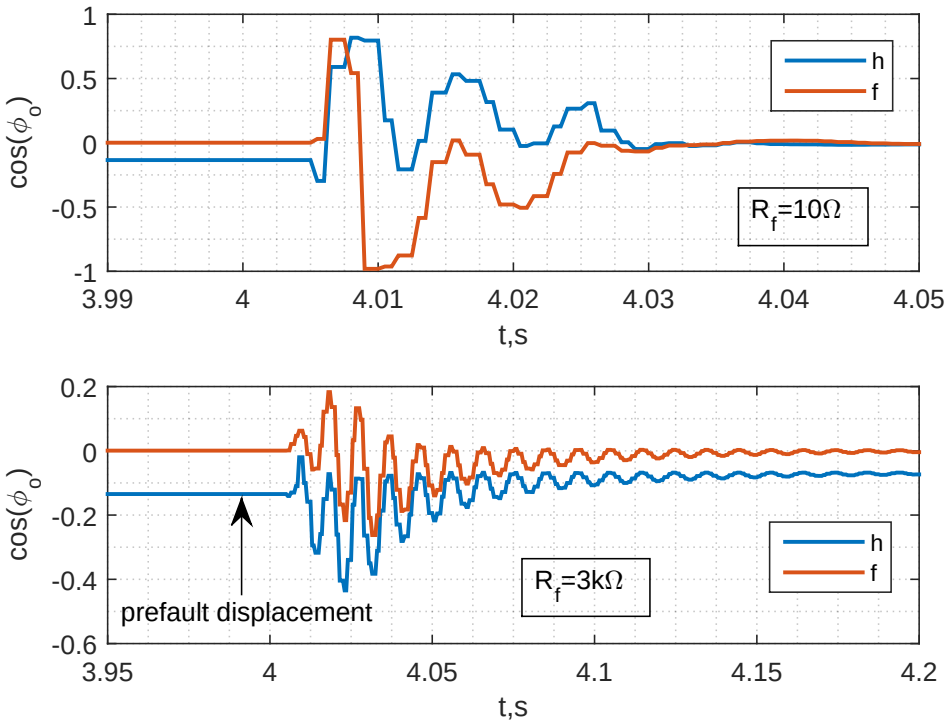

Figure 11: Transient characteristics of $\cos(\phi_0)$ for fault (phase a, $\Delta\bar{Y} = 2\%$, 90^0 inception angle) in feeder with cable and two fixed fault resistances $R_f = 3$ kΩ and 10 Ω.

predominantly in the positive half-plane. Thus, the CPS method works correctly for low-ohmic faults, see Fig.12. However, for high impedance faults, both phasors fall into the operating area (the dashed arrows).

Dependability of the method is improved if displacement tends to zero (operation point is close to resonance) because angle transients fall into the positive half-plane (as for low-ohmic faults); therefore, careful analysis of prefault conditions is important as in the case with steady-state methods.

To summarize, the transient methods are prone to malfunctioning in case of high impedance faults in compensated systems with significant electrostatic imbalance of phases and presence of underground cables. Finally, simulations have revealed that ground resistivity and load imbalance will not have significant

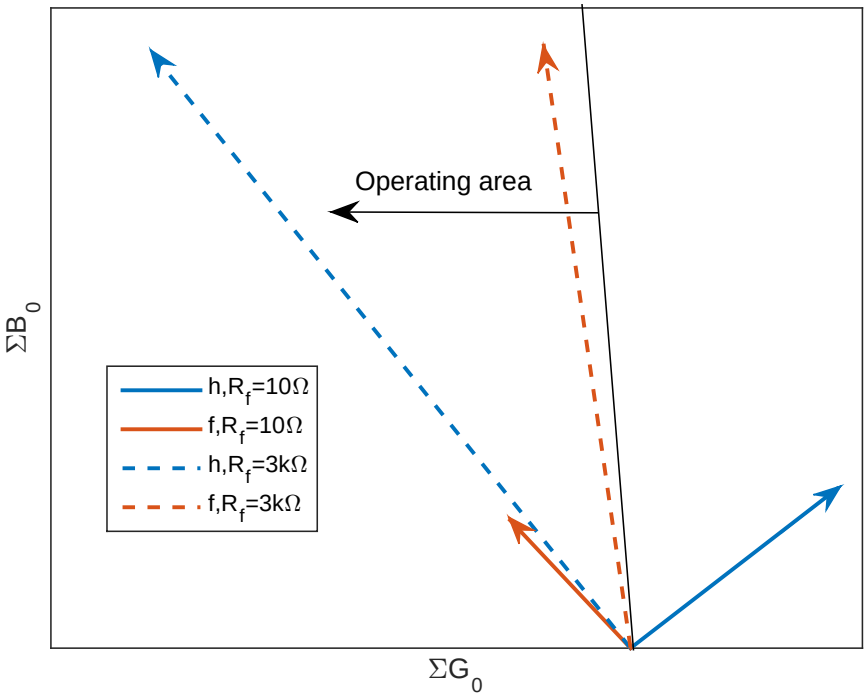

Figure 12: Cumulative admittance phasors calculated using (5) for fault (phase a, $\Delta\bar{Y} = 2\%$, 90^0 inception angle, $R_f = 3$ kΩ and 10 Ω) in feeder with cable.

impact on transient methods.

To conclude this section, we shall note that similar results will be obtained for models of networks with more complex topologies because they can be wrapped into two-feeder model (Fig.6), where the healthy feeder will perform a background network as it is shown in [8]. Furthermore, many methods were theoretically illustrated on two-feeder models and tested on complex models or on real measurements, e.g. [4].

6. Conclusion

The current work presents the most important methods (some of them can be founded in modern relays) for ground fault locating in distributed networks with resonant grounding and possible scenarios of their misoperations. The summary

is presented in Table 1. It indicates combination of the network parameters together with the worst fault conditions leading to inadequacy of the methods.

Table 1: Summary on the analyzed methods.

Method	Network conditions of inadequacy	The worst fault conditions
SS[1], $\lvert\bar{I}_0\rvert\cos(\phi_0)$ [2]	$\downarrow^2 G$, $\uparrow^3 \Delta\bar{Y}$, $\downarrow L$	HIF[4] in phase with the highest $\bar{Y}$ (among three phases).
SS, $\bar{Y}_0$ [4]	$\uparrow \Delta\bar{Y}$, prefault $\lvert\bar{I}_{0,f}\rvert > \lvert\bar{I}_{0,h}\rvert$	HIF in phase with the highest $\bar{Y}$.
T[5], $\cos(\phi_0)$ [19]	$\Delta\bar{Y} \neq 0$, fault inception angle.	HIF at 0^0 inception angle.
T, e_0 [23]	$\downarrow G$, $\uparrow \Delta\bar{Y}$, $\downarrow L$, wrong detection of fault inception time.	LOF[6] in phase with the smallest $\bar{Y}$.
T, i_0 [16], $\Sigma\bar{Y}_0$ [24]	Prefault $\lvert\bar{I}_{0,f}\rvert \gg \lvert\bar{I}_{0,h}\rvert$ (especially in mixed networks).	HIF in the feeder with large penetration of cables.

[1] steady-state, [2]insufficient/small value, [3] excessive/big value, [4] high impedance fault, [5] transient, [6] low-ohmic fault.

The protection based on steady-state signals is prone to the polarity disruption when a healthy feeder can be misjudged as a faulty. The obtained results clearly indicate how this effect depends on network and fault parameters. In many cases, this problem can be eliminated applying the parallel resistor; however, it provokes new challenges and finding of better solutions is still an ongoing process.

Utilization of transients to extract information is a more evident solution, however it requires more developed technologies (in terms of signal acquisition

and processing) and careful analysis in order to avoid incorrect decisions. The results show that the network electrostatic asymmetry, phase, fault impedance and inception angle have significant impact on the transient period compromising the algorithms. Other challenges might appear for cumulative criteria in networks with extensive penetration of cables, however mainly for high impedance faults. All these circumstances imply a need for further development of algorithms applicable for different network and fault types, as well as independent of information about system parameters, complex signal processing tools or additional equipment. It is advantageous to have universal settings for all relays in a system and fast operation time.

The further work will be dedicated to finding of an algorithm meeting the described requirements and handling all adverse effects performed in the current paper.

Appendix A. Model parameters

Table A.2: Elements of the model and their description.

Element	Description
Main grid	66 kV (line-to-line), short circuit capacity 250 MVA, 50 Hz
Transformer	20 MVA, 66/22 kV, leakage reactance 10%, copper losses 0.45%, tap 0.906 (primary side)
Overhead line (TL1 and TL2)	Hight 7.1 m, distance between 3 conductors (radius 10 mm, DC resistance 0.43 Ohm/km) 1.5 m (plane geometry), shunt conductance 10^{-8} S/km
Cable (part of TL1)	Depth 1 m, distance between phases 0.5 m (plane geometry); conductor: resistivity $4.2 \cdot 10^{-8}$ ohm·m, radius 5 mm; insulator: relative permittivity 5, radius 9 mm
Ground	resistivity 200 ohm·m
Load (100%)	interphase impedance $60 + j19$ Ohm

References

[1] X. Zhang, B. Xu, Z. Pan, P. Wei, "Study on single-phase earthed faulty feeder selection methods in non-solidly grounded systems", Third International Conference on Electric Utility Deregulation and Restructuring and Power Technologies, DRPT 2008, pp. 1836 – 1840, 2008.

[2] I. G. Kulis, A. Marusic, S. Zutobradic, "Insufficiency of watt-metric protection in resonant grounded networks", Eighth IEE International Conference on Developments in Power System Protection, DPSP 2004, volume 2, pp. 486 – 489, 2014.

[3] H. Ji, Y. Yang, H. Lian, S. Cong, "Effect on Earth Fault Detection Based on Energy Function Caused by Imbalance of Three-Phase Earth Capacitance in Resonant Grounded System", International Conference on Power System Technology, pp. 1 – 5, 2006.

[4] A.Wahlroos, J. Altonen, "Performance of novel neutral admittance criterion in MV-feeder earth-fault protection", 20$^{\text{th}}$ International Conference and Exhibition on Electricity Distribution – Part 1, CIRED, pp. 1 – 8, 2009.

[5] T. Henriksen, "Faulty feeder identification in high impedance grounded network using charge-voltage relationship", Electric Power Systems Research Journal, volume 81, issue 9, pp. 1832 – 1839, 2011.

[6] G. Druml, R. W. Klein, O. Seifert, "New adaptive algorithm for detecting low- and high ohmic faults in meshed networks", 20$^{\text{th}}$ International Conference and Exhibition on Electricity Distribution – Part 1, CIRED 2009, pp. 1 – 5, 2009.

[7] M. Loos, S. Werben, M. Kereit, J. C. Maun, "Detection of single phase earth fault in compensated network with C0 estimation", 22$^{\text{nd}}$ International Conference and Exhibition on Electricity Distribution (CIRED 2013), pp. 1 – 4, 2013.

[8] M. F. Abdel-Fattah, M. Lehtonen, "Transient algorithm based on earth capacitance estimation for earth-fault detection in medium-voltage networks", IET Generation, Transmission & Distribution, volume 6, issue 2, pp. 161 – 166, 2012.

[9] J. Berggren, L. Hammarson, "Novel method for selective detection of earth faults in high impedance grounded distribution networks", 18th International Conference and Exhibition on Electricity Distribution, pp. 1 – 4, 2005.

[10] K. Zhong-jian, L. Dan-dan, Z. Chao, L. Xiao-lin, "Research on the Fault Characteristic in Non-effectively Grounding Distribution Network with a Single-Phase-to-Earth Fault Based on Hilbert-Huang Transform", International Conference on Intelligent System Design and Engineering Application (ISDEA), volume 2, pp. 276 – 279, 2010.

[11] S. Hongchun, S. Shiyun, Q. Gefei, P. Shixin, "A new method to detect single-phase fault feeder in distribution network by using S-transform", IEEE 11th International Conference on Probabilistic Methods Applied to Power Systems (PMAPS), pp. 277 – 282, 2010.

[12] S. Zhang, H. Gao, M. Hou, Y. Sun, Z. Shao, J. Li, "Frequency spectrum characteristic analysis of single-phase ground fault in a Petersen-coil grounded system", 5th International Conference on Electric Utility Deregulation and Restructuring and Power Technologies (DRPT), pp. 369 – 374, 2015.

[13] K. Musierowicz, J. Lorenc, Z. Marcinkowski, A. Kwapisz, "A fuzzy logic-based algorithm for discrimination of damaged line during intermittent earth faults", IEEE Russia Power Tech, pp. 1 – 5, 2005.

[14] Y. Song, J. Liu, S. Yuan, C. Zhao, "Based on IAHP comprehensive evaluation method of the single-phase ground fault protection in cable distribution network", International Conference on Electrical and Control Engineering (ICECE), pp. 98 – 104, 2011.

[15] C. Zhongren, L. Weibo, H. Jian, "Single-phase grounding fault identification and fault line selection for compensation grid", 7th International Power Electronics and Motion Control Conference (IPEMC), volume 3, pp. 2290 – 2293, 2012.

[16] M. F. Abdel-Fattah, M. Lehtonen, "A transient fault detection technique with varying fault detection window of earth modes in unearthed MV systems", Power Quality and Supply Reliability Conference (PQ 2008), pp. 181 – 186, 2008.

[17] W. Y. Huang, R. Kaczmarek, "SLG Fault Detection in Presence of Strong Capacitive Currents in Compensated Networks", IEEE Transactions on Power Delivery, volume 22, issue 4, pp. 2132 – 2135, 2007.

[18] Y. Qi, Z. Wen, H. Jia, "Distribution Network Fault Location Algorithm Based on Zero-Sequence Current Phase", Spring Congress on Engineering and Technology (S-CET), pp. 1 – 4, 2012.

[19] P. Balcerek, M. Fulczyk, J. Izykowski, E. Rosolowski, P. Pierz, "Centralized substation level protection for determination of faulty feeder in distribution network", IEEE Power and Energy Society General Meeting, pp. 1 – 6, 2012.

[20] X. Yongduan, X. Bingyin, C. Yu, F. Zuren, P. Gale, "Earth fault protection using transient signals in non-solid earthed network", International Conference on Power System Technology (PowerCon 2002), volume 3, pp. 1763 – 1767, 2002.

[21] X. H. Zhang, H. X. Ha, Z. C. Pan, B. Y. Xu, "Grounding faulty line selection in non-solidly grounded systems using transient energy", International Power Engineering Conference (IPEC 2007), pp. 1147 – 1150, 2007.

[22] L. Jian, H. Jianjun, Z. Hongwei, Y. Hua, Z. Jie, L. Lei, W. Rui, "Fault Line Selection Based on Zero Sequence Power Direction of Transient Fun-

damental Frequency in MV Network Grounded with Arc Extinguishing Coil", International Conference on Power System Technology, pp. 1 – 4, 2006.

[23] M. Loos, S. Werben, M. Kereit, J. C. Maun, "Fault direction method in compensated network using the zero sequence active energy signal", IEEE EUROCON, pp. 717 – 723, 2013.

[24] A. Wahlroos, J. Altonen, "Application of novel multi-frequency neutral admittance method into earth-fault protection in compensated MV-networks", 12th IET International Conference on Developments in Power System Protection (DPSP 2014), pp. 1 – 6, 2014.

[25] Z. Chen, H. Wang, F. Chen, "Research on Damping Ratio and Off-Resonant Degree of Compensation Network", Asia-Pacific Power and Energy Engineering Conference (APPEEC), pp. 1 – 4, 2011.